Provenance analysis for submarine fan sandstones of Huangliu Formation, Dongfang 13 gas field in Yinggehai Basin, South China Sea

Yintao Huang[1,2], Guangqing Yao[2,*], Fengde Zhou[3]

[1]*Faculty of Resource Environment and Tourism, Hubei University of Arts and Science,Xiangyang, China*
[2]*Faculty of Earth Resources, China University of Geosciences, Wuhan 430074, China*
[3]*School of Earth Sciences, University of Queensland, Brisbane QLD 4072, Australia*
Corresponding author: cug218@hotmail.com

Abstract

The reservoir in the upper Miocene Huangliu Formation, in the Yinggehai Basin, is composed of submarine fan deposits with burial depths from 2600m to 3500m. This paper presents an integrated method in provenance analysis by using data of petrography, heavy mineral assemblages, and geochemical compositions. The analysis produced a number of key results. First, two provenances exist, one in the west and the other in the east. Second, the submarine fan sandstone exhibits low percentages of zircon, tourmaline and garnet, whereas the neritic sandbar rocks exhibit high percentages of zircon, tourmaline and leucoxene, and low percentages of magnetite and garnet. Third, the Chemical Index of Alteration (CIA) values and Rb/Sr ratios of the submarine fan sandstone indicate moderate weathering intensity in the source region. SiO_2/Al_2O_3 ratios indicate moderate sediment maturity. Similar rare earth element patterns of the submarine fan sandstone samples from three wells indicate a common provenance. Th-Sc, Co/Th-La/Sc and REE patterns point to derivation from felsic source rocks. Fourth, the integrated method and comparison of REE patterns of the submarine fan sandstone with that of possible adjacent source rocks indicates that the submarine fan sandstone most probably derived from the western Kuntum uplift. It is concluded that the integration of petrological composition of the sandstone, the heavy mineral assemblage and major and trace elements geochemistry is useful for provenance identification.

Keywords: Geochemistry; heavy minerals; provenance; submarine fan; Yinggehai Basin.

1. Introduction

Provenance analysis is used to deduce the characteristics of source areas based on the compositional and textural properties of sediments and information supplemented from other evidence (Pettijohn *et al*., 1987). Traditional methods are mainly based on the assemblage of heavy minerals (Morton, 2005; Fu *et al*., 2013), the petrographic-mineralogical method (Dickinson, 1985), chemical and radiometric ages of single mineral grains (Morton, 2005) and whole-rock chemical composition (Bhatia, 1983; Taylor & McLennan, 1985; Roser & Korsch, 1988; McLennan *et al*., 1993). Moreover, the major and trace element compositions provide useful information on provenance, weathering conditions and tectonic settings for siliciclastic sediments (Armstrong-Altrin *et al*., 2012; 2014; 2015). Most studies use only one method, such as petrology or whole-rock chemistry. However, the mineralogical and chemical compositions of sedimentary rocks are affected by many factors, e.g., type of source rock, weathering conditions in the source area, climate conditions, transportation distance, burial history and diagenesis (McLennan *et al*., 1993; Moosavirad *et al*., 2011). Hence, traditional petrographic analysis has limitations in provenance analysis (McLennan, 1989; Nesbitt & Young, 1996). In contrast, an integrated method using the mineralogical components of sandstone, heavy mineral assemblages, and geochemical characteristics can be used to analyze provenance and tectonic settings (El-Bialy, 2013; Zaid, 2013; Saminpanya *et al*., 2014).

The Yinggehai Basin in the northwestern South China Sea is a target for the petroleum industry. The sandbody of member #1 in the late Miocene Huangliu formation was recently discovered as a potential for oil and gas production in the central depression of this Basin. Two sedimentary systems, a channel-lobe complex of submarine fan and neritic sandbar, were recognized (Xie *et al*., 2012; Zhang *et al*., 2013). The submarine fan system developed on the continental shelf and is referred to as a "shallow marine submarine fan" (Sun *et al*., 2014). Research shows an inner basin slope break in the continental shelf due to differential subsidence of the continental shelf (Sun *et al*., 2014; Wang *et al*., 2015). The fine-grained sediments were transported to the margin of the inner basin slope break, forming the thick delta-front sand body (Sun *et al*., 2014; Wang *et al*., 2015). The delta-front sand body eventually slumped, forming a sediment gravity flow deposition in the Dongfang area due to the sea-level falling and an abrupt increase of the slope ratio (Sun *et al*., 2014; Wang *et al*., 2015).

Although many authors have studied the reservoir characteristics, genetic mechanism, diagenesis, and overpressure of the submarine fan sandstone (Pei *et al*., 2011; Zhang *et al*., 2013; Wang *et al*., 2015), its provenance is still unclear because the area is located near mud diapir belts (Xie *et al*., 2012; Zhang *et al*., 2013). Xie *et al*. (2012) and Zhang *et al*. (2013) assumed that the possible source areas were the western Kuntum uplift, the northwestern Red River and eastern Hainan Island. Very few studies examine the geochemical provenance data of sandstone in this area. Therefore, the aims of this study were (1) to evaluate the compositional differences of the sandstones in the submarine fan system and the neritic sandbar; (2) to evaluate the weathering condition of the submarine fan sandstones; and, (3) to identify the provenance based on the petrological composition of the sandstone, the heavy mineral assemblage, and major and trace elements geochemistry.

2. Geological setting

The Yinggehai Basin, with an area of 12.17×10^4 km^2, extends in a northwest to southeast direction. It is located between the eastern Hainan paleo-uplift (Hainan Island) and the western Kuntum paleo-uplift. This basin includes three first-order tectonic units, the Yingdong slope, the central depression and the Yingxi slope (Fig. 1a). Previous studies reported that a series of mud diapir belts were generated by right-lateral strike-slip tension during the Miocene-Pliocene time (Zhang *et al*., 1999; Hao *et al*., 2003; Pei *et al*., 2011). The mud diapir belts are classified as secondary tectonic units in the center of the central depression.

The study area is the Dongfang 13 gas field, located in the northern part of the central mud diaper belts (Figures 1a and 1c), which produces gas from deep strata (Fig. 1b). The Dongfang 1-1 gas field is also present in this area. It was discovered during the 1990s. It produces gas from shallow strata (Fig. 1b) in a normal temperature and pressure system, whereas the deep strata are in a high temperature and pressure system (Pei *et al*., 2011). Four formations are present in the Dongfang 13 gas field, namely the Sanya, Meishan, Huangliu and Yinggehai formations from bottom to top (Fig. 1b). Member #1 of the Huangliu formation includes two gas layers: I and II. In this area, 20 wells have been drilled, and sandstone thickness ranges from 10m to 76m and 34m to 105m for gas layers I and II, respectively.

The depositional system from most of the wells were recognized as the submarine fan system except for two wells (A-3 and C-12) which were neritic sandbar (Zhang *et al*. 2013) (Fig. 1c). Many rivers, e.g. the Red River and the Blue River, were located in the Yingxi slope and flowed into the Yinggehai basin from the northwest or west (Xie *et al*., 2012; Zhang *et al*., 2013). In contrast, the Yingdong slope has a major fault with a small-size neritic sandbar of mainly argillaceous siltstone (Xie *et al*., 2012; Zhang *et al*., 2013).

3. Samples and experimental methods

In this study, 420 casting thin sections (impregnated with blue resin) were analyzed from gas layer #1 and #2 of 13 wells. The amounts of detrital components, as well as the textural modal grain size and sorting parameters, were determined by counting at least 300 points as prescribed by the Gazzi-Dickinson method (Dickinson, 1970). The categories were for total quartz (monocrystalline quartz and polycrystalline quartz), total feldspar (potash feldspar and plagioclase), total lithics (igneous (Lv), sedimentary (Ls), metamorphic (Lm)), and heavy minerals.

Heavy mineral data from 23 wells were used—12 wells inside and 11 wells outside the main study area (from Zhong *et al*., 2013). The core samples for heavy mineral analysis were firstly crushed, acidized by 10% concentration of hydrochloric acid and dried at 105°C. Then the samples were immersed and cleaned in water to remove clay that might have adhered to the grain surface. Thereafter, the 63–250μm faction was selected by sieving, and heavy minerals were separated by heavy liquid bromoform with a density of 2.80 g/cm^3. The heavy minerals were then identified with a polarizing microscope. The grain morphology and texture were examined with a scanning electron microscope (SEM; Quanta 600).

For analysis of the whole-rock geochemical composition, 28 fresh core samples were collected from the submarine fan sandstones. Those samples were from the three cored wells, A-2, A-6 and A-8 (Fig. 2), that were allowed to be sampled. Note that there is no clear age information of the samples in this study. The lithology is mainly fine sandstone and silt to fine sandstone. The samples were analyzed by the Test Center of Ministry of Land and Resources in Wuhan, China according to the "China laboratory tests of geology and mineral resources and the quality control standard: mineral rock analysis" (DZ/T0136.2—2006). The samples were crushed and powdered using an agate mortar to less than mesh No. 200 (around 0.07mm). Major elements were measured using X-ray Fluorescence Spectrometry (XRF-1800). Fused beads were prepared from each calcinated sample by means of a lithium tetraborate flux for X-ray fluorescence analyses. The powdered samples were then heated to 110° C for 6 h followed by heating in a muffle furnace at 1000° C for two hours to determine loss on ignition (LOI). Trace elements and rare earth elements (REEs) were measured by inductively coupled plasma mass

spectrometer (Thermo Elemental-X7 Quadrupole ICP-MS). The analytical precision for major elements, trace elements, and REE is generally better than 5%.

The Chemical Index of Alteration (CIA) is used to assess the degree of chemical weathering (e.g. Nesbitt and Young, 1982). The value of CIA can be calculated by molecular proportions,

the formula $CIA=[Al_2O_3/(Al_2O_3+K_2O+Na_2O+CaO^*)]\times100$, where CaO^* represents CaO in silicates only. In this study, CaO values were accepted only if $CaO<Na_2O$; when $CaO>Na_2O$, it was assumed that the concentration of CaO was equal to that of Na_2O (McLennan *et al.*, 1993).
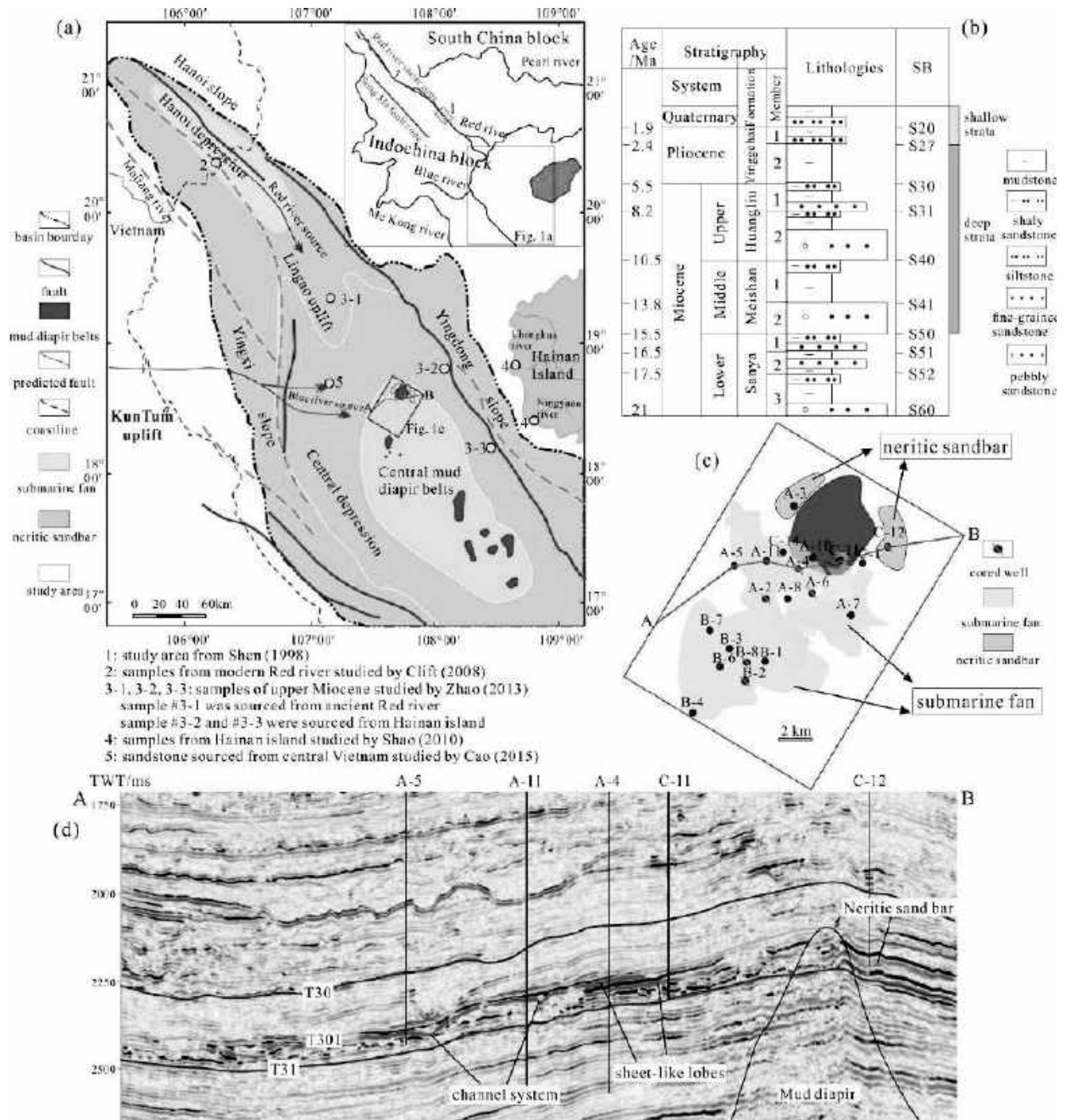
Fig. 1. (a) Locations of Yinggehai basin and this study area, (b) stratigraphy, (c) location of wells in study area (the range of submarine fan and neritic sandbar is from Zhang *et al.*, 2013) and, (d) one seismic section from the study area in Yinggehai Basin (Fig. 1a is from Zhang *et al.*, 2013). Note SB: sequence boundary in Fig. 1b.
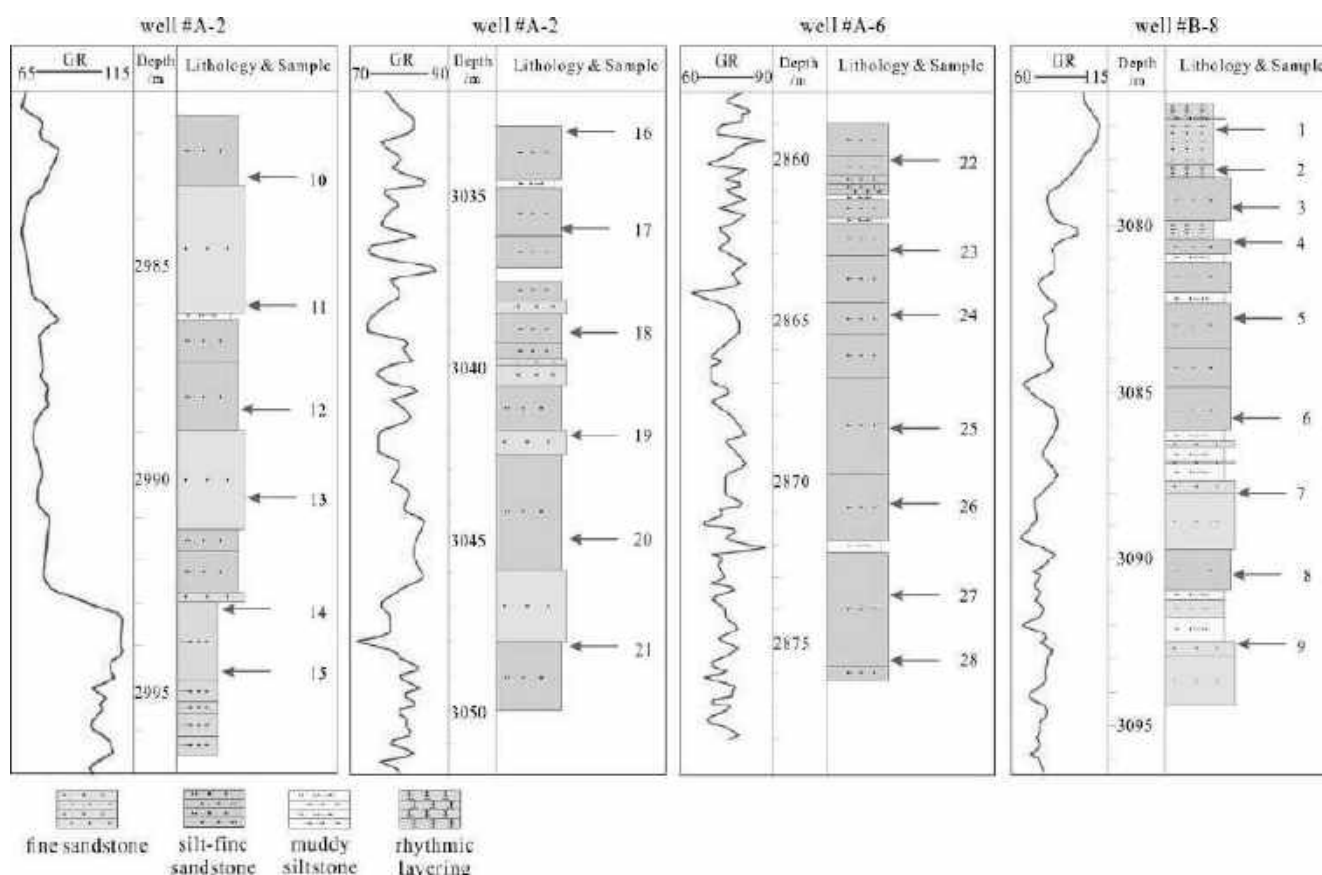
Fig. 2. Lithology and locations of sandstone samples collected for geochemistry analysis (Note: rhythmic layering means alternation of sandstone and mudstone with thickness of 12-cm; GR means gamma-ray logging in API).

4. Results

4.1. Reservoir petrography

4.1.1. Sandstone composition

In this study area, the main lithology was moderately sorted, fine-grained sandstone to siltstone (Table 1) with sub-angular to sub-rounded grains (Figs. 3a-3b). The detrital grains included mean values of 46-62% quartz, 4-9% feldspar, and 2-14% lithic fragments. The content of monocrystalline quartz (average is 51%) was much higher than for polycrystalline quartz (average is 5%), and the content of potassium feldspar (average is 6%) was higher than for plagioclase (average is 1%). Lithic fragments (average is 10%) included metamorphic, sedimentary, and igneous lithic fragments. Heavy minerals like magnetite were also presented (Fig. 3c). In analysis, 43% of these casting thin sections were sublitharenite and 40% were feldspathic litharenite (Fig. 4).

The sandstone from the submarine fan system was mainly sublitharenite with high feldspar and lithic-fragment content, high textural maturity, low shale content (average is 4%), and high thin-section porosity (average is 18%). The sedimentary rocks from the neritic sandbar were determined to be mainly subarkose to-quartz siltstone with low feldspar (average is 5%) and lithic-fragment content (average is 3%), high compositional maturity, high shale content (average of 19%), and low thin-section porosity (average is 8%). Note that the proportion of secondary porosity may affect the resulting mineralogical and chemical composition. However, in this study area, secondary porosity only accounted for little proportion of the total thin-section porosity (approximate 5-10%), which indicates an ignorable effect.

The neritic sandbar is situated in the eastern mud diapir belts, e.g. well C-12, and the submarine fan sedimentary system is situated in the western mud diapir belts. However, the major constituents of sandstone do not provide a sufficient evidence to identify the provenance because they are ubiquitous (Weltje & Von Eynatten, 2004). Furthermore, the composition of sandstone, the textual and mineralogical maturity, and the shale content are affected by the transportation distance.

The constituent of siltstone and sandstone may be affected by ocean currents in this study area. Therefore, the different compositions of rocks from the neritic sandbar and submarine fan system only indicate that these two sedimentary systems have different provenance (Table 1).
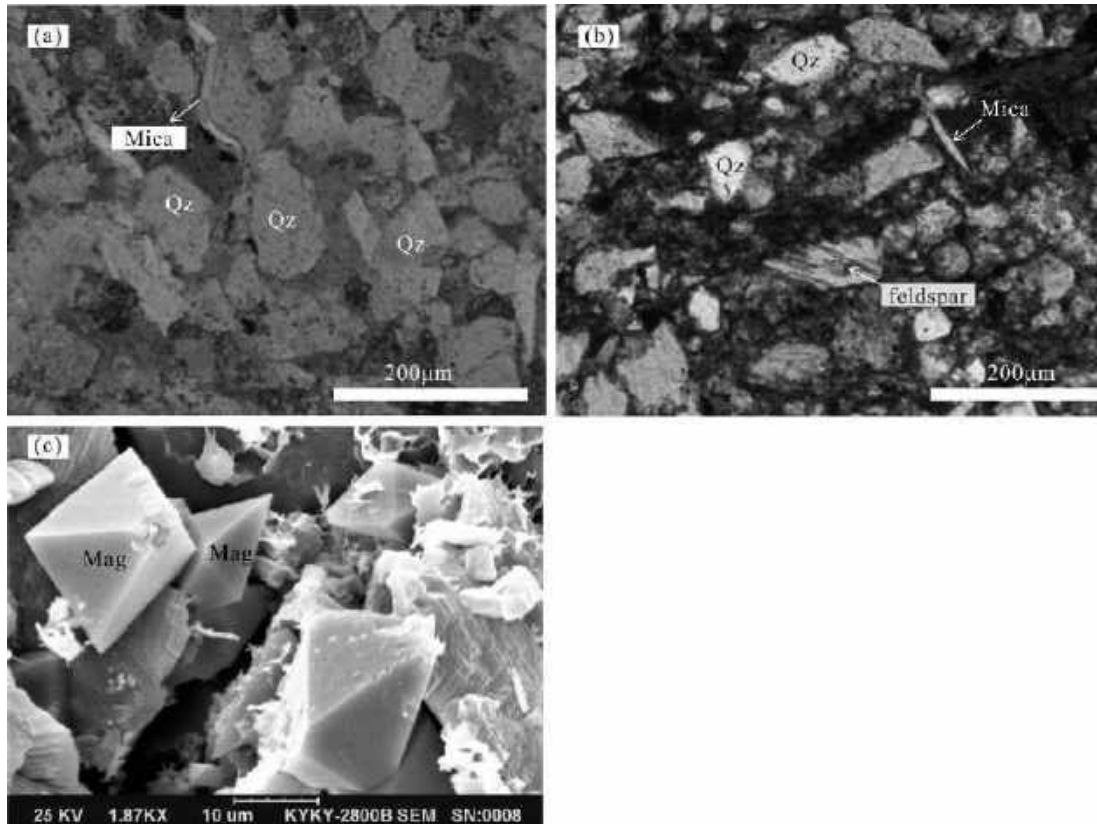
Fig. 3. Microphotographs from thin sections (a and b) and scanning electron microscope (SEM; c) of submarine fan sandstone and neritic sandbar. (a) sub-angular to sub-rounded quartz grains (Qz) in submarine fan sandstone with low shale content (1%), under plane-polarized light, well #A-2,
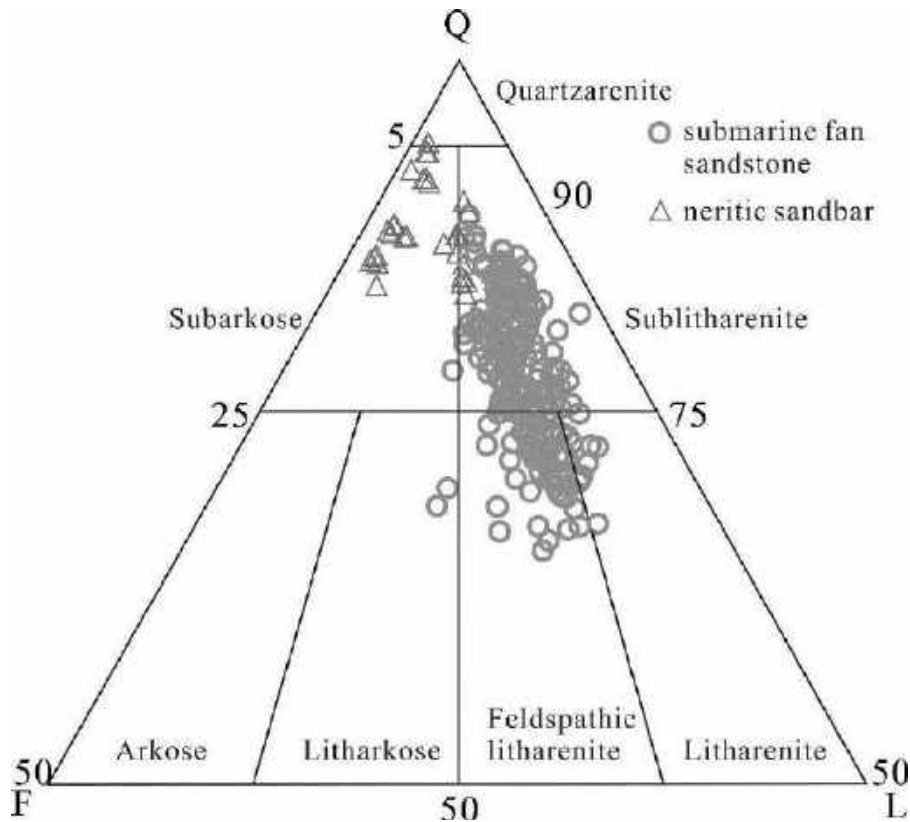
Fig. 4. Classification of sandstone and siltstone in this study area. The discrimination fields are after Folk (1974).

Table 1. Components of sandstone from the study area.

Microfacies	Wells	N	Gas layer	Thickness /m	Thin-section porosity /%	Cement content /% calcite	Cement content /% ferrocalcite	Qt Qm	Qt Qp	F K	F P	Lv	Lm	Lt	Ls	HM	Texture maturity Shale content/%	Texture maturity	Composition maturity index	Composition maturity	Displacement pressure /MPa	Median pressure /MPa	Average pore-throat radius /μm	Rock type
Neritic sand bar	C-12	13	II	10	5	6	2	59	2	4	0	3	1	1	0	1	17	low	7	high-very high	/	/	/	subarkose-quartz siltstone
	A-3	16	I	18	9	3	2	56	2	3	1	2	0	0	0	1	20	low	9	high-very high	3.6	22.59	0.07	Subarkose (siltstone)
Submarine fan	A-2	30	I	15.5	20	2	1	54	3	4	0	1	2	6	1	1	2	high	5	high	0.42	2.05	0.57	Sublitharenite (vf)
	A-2	25	II	38.8	19	3	1	55	5	4	0	2	2	6	1	1	2	high	5	high	0.41	1.15	0.73	Sublitharenite (vf)
	A-4	20	I	23.4	17	4	2	50	7	3	1	2	2	9	0	2	1	high	4	moderate	0.19	0.74	1.44	Sublitharenite (f)
	A-5	32	I	28.9	13	1	1	51	7	7	1	3	3	8	0	1	6	moderate	3	moderate	0.36	2.25	0.66	Sublitharenite (f)
	A-6	16	II	44.2	21	2	1	50	8	5	1	1	1	7	0	2	1	high	4	moderate	0.37	1.33	0.74	Sublitharenite (vf)
	A-7	16	I	20	22	2	1	52	4	6	0	2	2	7	0	1	1	high	4	moderate	0.17	3.18	1.41	Sublitharenite (vf)
	A-7	15	II	37	18	3	1	54	3	5	0	2	2	10	0	1	1	high	3	moderate	0.17	0.99	1.54	Sublitharenite (vf)
	A-8	22	I	8.6	14	3	1	50	4	4	0	2	2	11	0	1	7	moderate	3	moderate	/	/	/	Sublitharenite (f)
	A-8	20	II	18.6	17	3	1	50	4	5	1	2	2	12	0	1	3	high	3	moderate	/	/	/	sublitharenite (vf)
	B-1	22	II	20	12	1	1	55	7	8	1	2	2	10	1	1	1	high	3	moderate	/	/	/	feldspar litharenite (vf)
	B-2	43	II	10.3	11	3	0	53	7	6	0	3	3	7	0	2	8	low	4	moderate	0.17	5.72	1.39	Subarkose (vf)
	B-4	31	I	20	22	4	2	42	4	6	1	2	2	11	0	0	3	moderate	2	moderate	0.11	1.64	2.35	feldspar litharenite (f)
	B-6	22	I	10	22	3	1	43	6	5	0	3	3	10	0	1	3	high	3	moderate	0.71	0.19	4.48	Sublitharenite (f)
	B-6	16	II	8	18	3	2	45	5	5	1	3	3	10	0	1	6	high	3	moderate	0.29	2	1.43	Sublitharenite (f)
	B-8	61	I	29.8	20	1	2	49	6	6	1	1	1	10	0	2	2	high	3	moderate	0.1	0.58	3.31	feldspar litharenite (f)

/ indicating no data; composition maturity index=Qt/(F+R); N=number of sections for each well

Qt= total quartz grains; Qm= monocrystalline quartz grains; Qp= polycrystalline quatz grains; feldspar (F) = potash feldspar (K)+plagioclase (p); Lt= total lithics; Lv= igneous lithic; Lm= metamorphic lithic; Ls= sedimentary lithic; HM= heavy minerals; N= number of sections; vf= very fine-grained sandstone; f= fine-grained sandstone

4.1.2. Assemblage of heavy minerals

In this study, more than 20 types of heavy minerals were recognized. In addition, zircon, tourmaline, garnet, magnetite, hematite-limonite and leucoxene occur in almost all samples. The average percentages of these six minerals was 85%, and the percentage of other single heavy mineral was less than 1%.

Wells located on the Yingdong slope have high percentages of zircon, tourmaline and leucoxene, but low percentages of magnetite and garnet. For example, in well #HK17-1-1, the percentage of leucoxene is 35%; the percentages of zircon

and tourmaline were greater than 10%, and the percentage of garnet was less than 10% (Fig. 5). This is similar to recent sediment from the Hainan Island (Zhong *et al*., 2013). However, the heavy minerals for the samples from Dongfang area had different characteristics. For example, in well # C-1, the percentages of tourmaline and zircon were less than 10% (Fig. 5). Finally, the submarine fan sandstone had lower percentages of zircon and tourmaline, but higher percentages of magnetite and garnet than the neritic sandbar sediment (Fig. 5).
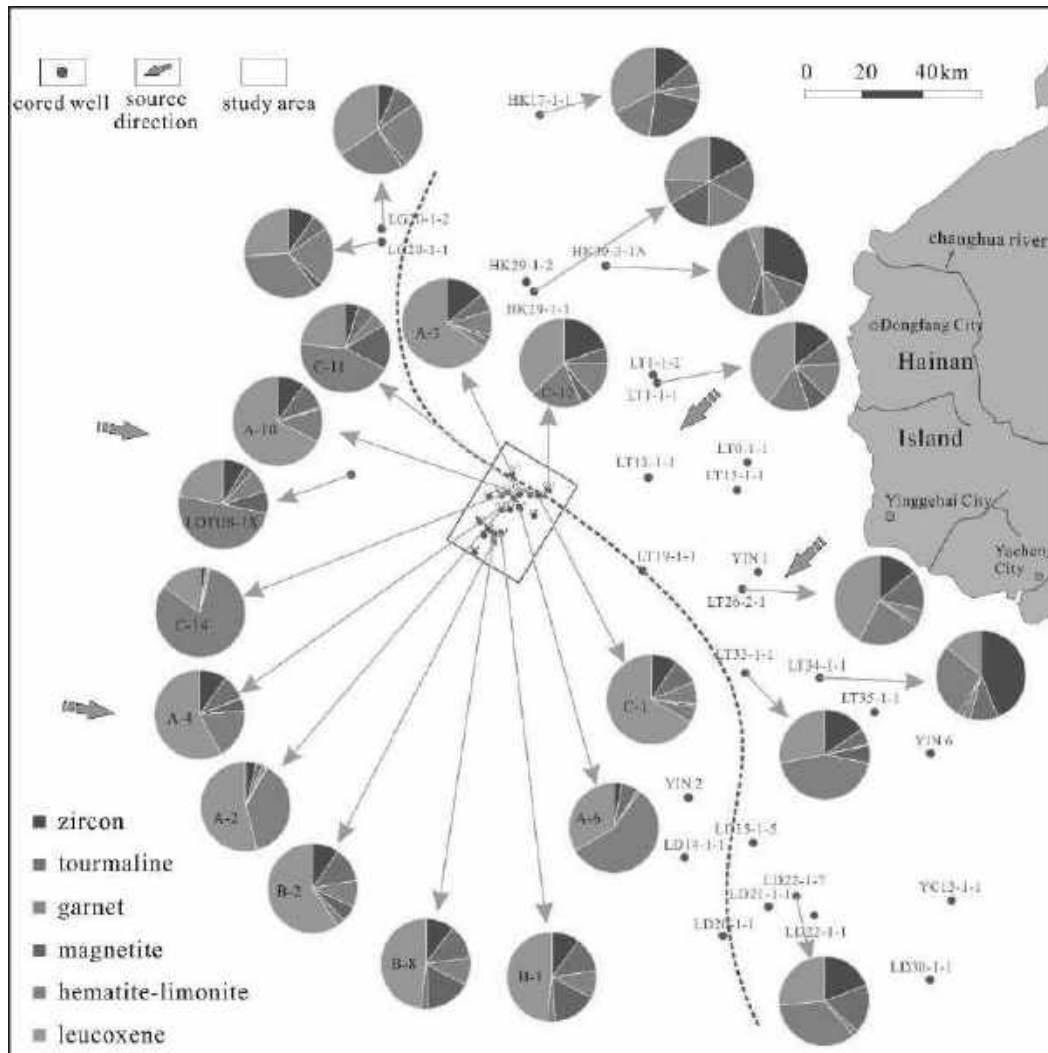
Fig. 5. Distribution of the six heavy minerals in the study area. (Data outside the study area is from Zhong *et al*., 2013). The red dotted line means the possible boundary of the western source and eastern source.

4.2. Geochemistry of submarine fan sandstones

4.2.1. Major elements

Major elements of 28 samples from Huangliu formation showed variable content in SiO_2 (63~83%), Al_2O_3 (7~13%), CaO (1~6%), MgO (1.0~2.2%), K_2O (1.7~2.7%), Na_2O (0.8~1.4%), FeO (2.1~4.2%), Fe_2O_3 (0.3~1.7%). Generally,

the content of other single major elements was less than 1% (TiO_2, P_2O_5, MnO) (see Table 2). Most major elements had positive correlation coefficients with Al_2O_3, except SiO_2 (Table 3). From fine-grained sandstone to very fine-grained sandstone, the content of SiO_2 decreased, whereas the contents of Al_2O_3, K_2O and TiO_2 increased slightly. The average content of SiO_2, Al_2O_3, K_2O and TiO_2 in fine-

grained sandstone (sample # 3-9; table 2) was 78.8%, 7.4%, 1.8% and 0.5%, respectively. However, the average content for those in very fine-grained sandstone was 72.6%, 9.3%, 2.1% and 0.7%, respectively. The values of Fe_2O_3/K_2O, SiO_2/Al_2O_3 and Al_2O_3/TiO_2 ranged from 1.7-2.4 (average is 2.0), 4.8-12.4 (average is 8.7), and 11 to 17 (average is 14.5), respectively. The values of SiO_2/Al_2O_3 ranged from 4.8-12.4 (average is 8.7). The CIA values of submarine fan sandstone ranged from 57 to 69 (Table 2) with an average of 60, and the CIA values of most samples were less than 65. Based on Fe_2O_3/K_2O and SiO_2/Al_2O_3 ratios, most of

the submarine fan samples can be chemically classified as litharenite (Fig. 6).

Positive correlations exist between Al_2O_3 and K_2O (r=0.73), TiO_2 (r=0.88), and MgO (r=0.84). This indicates that K-bearing minerals have a significant influence on the distribution of Al. The abundance of these elements is primarily controlled by the content of clay minerals (McLennan *et al.*, 1993; Akarish & El-Gohary, 2008; Armstrong-Altrin, 2004). Negative correlations between SiO_2 and other major elements indicate that SiO_2 is mainly bound in quartz (Akarish & El-Gohary, 2008; Zaid, 2013).
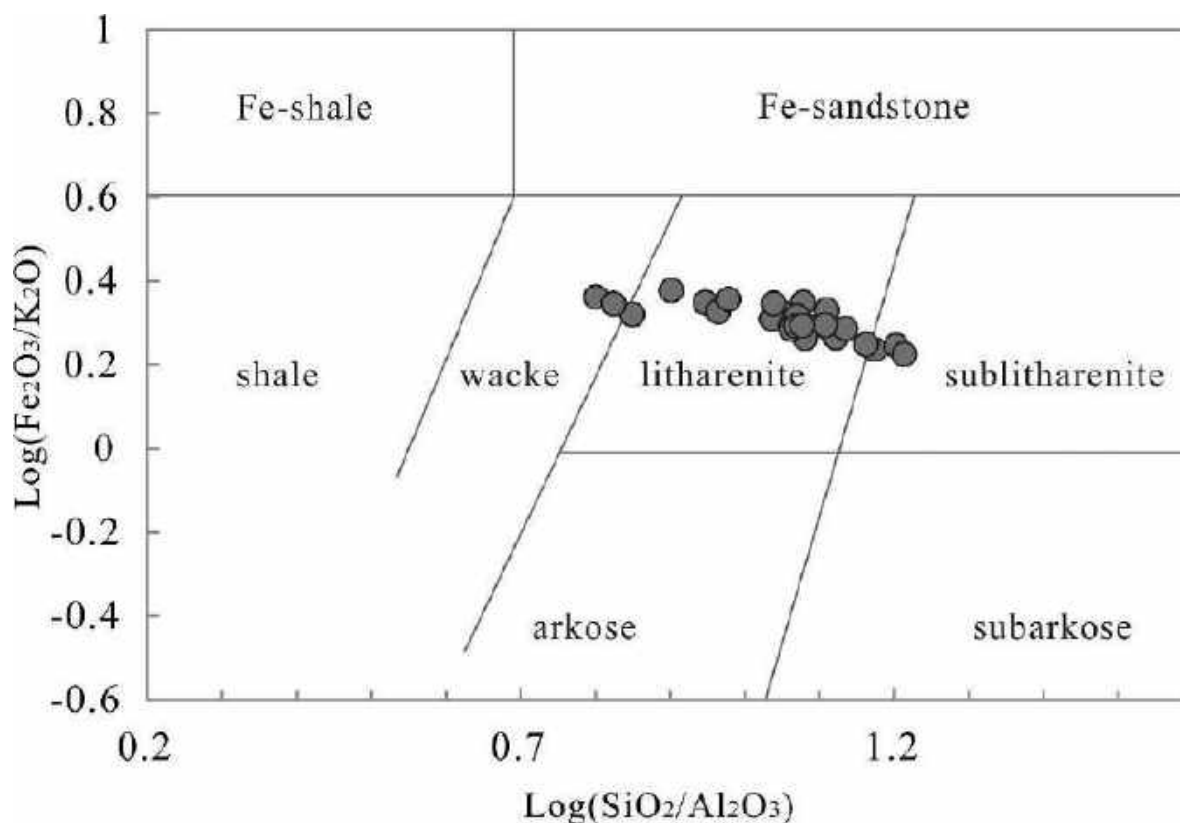
Fig.6. Classifications of sandstone based on the composition of major element (after Herron, 1988).

4.2.2. Trace elements

The samples had high contents of Ba, Sr, and Zr with average values of 482, 119, and 280 ppm, respectively (Table 2). The average contents of Rb, V, Cr, B and Ni were 75, 60, 57, 17, 56 and 21 ppm, respectively (Table 4). The compatible ferromagnesian trace elements (Ni, Cr, Sc, and V) and the large ion lithophile elements (LILEs; Rb, Ba, K and Sr) were depleted relative to the upper continental crust (UCC; Table 4). The Zr concentration varied from 168 to 888 ppm with average of 280 ppm which was higher than for UCC (=193ppm). The REE patterns were generally parallel to sub-parallel with light REE enrichment, similar to UCC (Fig. 7). The ratios of LREE/HREE, $(La/Yb)_N$, and $(Gd/Yb)_N$ ranged from 7.611.1- (average is 9.3), 7.2-13.6 (average

is 11.0) and 1.3-2.1 (average is 1.8), respectively. Eu/Eu* was 0.48-0.70 (average is 0.64), which was less than UCC (0.70). In this study, Cr ranges were from 48 to 83 ppm with averages of 57 ppm. Ni ranges were from 15 to 29 ppm with averages of 21 ppm. Ranges for Cr/Ni were from 2.2 to 3.9 with averages of 2.7 (Table 4), and Th/Sc ranged from 0.90 to 2.25 with averages of 1.28. These results were higher than for the UCC (Table 4; Fig. 8a). The Rb/Sr and Co/Th values for submarine fan sandstones ranged from 0.24-0.88 (average is 0.65) and 0.5-1.3 (average is 0.9) (Table 4). The samples displayed higher total REE contents (128-381 ppm, average=176 ppm) than UCC (Table 4).